

PROJECT X H- INJECTION DESIGN HISTORY AND CHALLENGES*

D.E. Johnson, A.I. Drozhdin, I. Rakhno, L.G. Vorobiev, Fermilab, Batavia, Illinois, U.S.A.
T. Gorlov, ORNL, Oak Ridge, Tennessee, U.S.A.; D. Raparia, BNL, Upton, New York, U.S.A.

Abstract

One of the initial motivations for replacing the aging Fermilab Proton Source was to support the 120 GeV Neutrino program at the 2 MW level while supporting a broad 8 GeV Physics program. Over the years the design parameters of the new Proton Source have evolved from the 2005 Proton Driver configuration of a 2MW 8 GeV pulsed H- linac injecting directly into the Main Injector or Recycler; to a 2MW 2 GeV CW linac supporting a 2 GeV Experimental Program while injecting into a new 2 to 8 GeV Rapid Cycling Synchrotron which would then supply protons to the Recycler. The current design parameters of the project include a 3 GeV CW linac accelerating up to 1 mA (average) H- and a 3 GeV Experimental Area with the connection to the Main Injector Complex as an upgrade. Whether the upgrade path includes a new 6(or 8) GeV CW or pulsed linac, or 3 to 8 GeV RCS and the ultimate linac current, remains to be determined. The basic issues of injection insertion design, foil and laser stripping options, foil survivability and loss issues will be analysed in context of the present options. Both analytical estimates and simulation results will be discussed.

INTRODUCTION

Current Configuration

The current accelerator configuration [1], as documented in the Reference Design Report [2], consists of

- a 3 GeV CW superconducting linac accelerating 1 mA of H⁻ in a 325 MHz bunch structure,
- a 3 GeV H⁻ transport line to simultaneously deliver MW range beam power to at least three experiments with variable bunch configurations,
- a 3 to 8 GeV Rapid Cycling Synchrotron (RCS) running at 10 Hz with H⁻ multi-turn injection,
- a 8 GeV proton transport line from the RCS to the Recycler where 6 batches are accumulated for single turn injection into the MI for the LBNE program.

Path Forward

It is recognized that the RCS configuration does not lead to an upgrade path toward muon source for a possible Muon Collider and/or Neutrino Factory at the 4 MW power level. Therefore, an R&D program to establish a self-consistent design of a 3 to 8 GeV superconducting linac, based upon 1.3 GHz SCRF cavity technology, injecting into the Recycler (RR) or directly

into the Main Injector (MI), is being developed. Implicitly included in this plan is the development of a self-consistent design for H- injection into the Recycler or Main Injector.

High Energy Linac Design

Two design options for a high energy (HE) linac fed from the 3 GeV CW linac are being investigated: 1) a pulsed linac operating at ~ 10 Hz with a range of macro beam pulse lengths between 1 and 4 ms and average beam currents between 4 and 1 mA, and 2) a low current CW linac with a beam current ~ 1 mA and macro beam pulse of ~26ms.

Design Challenges

This report will utilize the injection system design previously reported [3-7] and focus on potential options for the development of two techniques for implementing H-injection. Carbon foil stripping has been the main stay of multi-turn H- injection for the last several decades. It is currently the default technique. Recently, the technique of laser assisted stripping has gained much attention as a technique for H- injection without the use of physical stripping foils. We will discuss the status of each in relation to their impact on the choice of HE linac type.

CARBON FOIL INJECTION

The basic issues related to carbon stripping foils are: foil lifetime, losses associated with single coulomb scattering and nuclear interactions, and emittance growth due to multiple coulomb scattering.

The interaction of the injected H- and circulating beam impact the foil life time through heating due to energy deposition and radiation damage of the carbon crystalline structure [8] and create particle losses through scattering and nuclear interactions. The key is to minimize the number (and density) of foil traversals through the choice of injection lattice, ring lattice, painting algorithm, and foil size and geometry.

We report on the current status of optimization of H-injection into the RR/MI. Here, we look at the foil traversal rate and density for a range of linac currents from 1mA to 4 mA and pulse lengths from 1 to 4 ms for two coil configurations.

The short linac pulse lengths require six injections to accumulate the required charge (26 mA-ms). The circulating beam is removed from the foil between injections so the foil cools down between injections. Additionally, the instantaneous intensity from the injected beam is a factor of 6 less than that from a high current short pulse single injection, as in the Proton Driver [4].

For both the RR and MI, each 1 ms of injection requires ~90 turns with the complete injection time for six

*Work supported by U.S. Department of Energy under the contract No. DE-AC02-76CH03000.

#dej@fnal.gov

injections on the foil of ~540 turns. Total turns on injection foil scales linearly with injection time.

Number of Foil Traversals

Two conditions for twiss parameter mismatch have been identified which will reduce foil hits by circulating beam in phase space painting. [9] We satisfy these two conditions by having both the injected and circulating beam with $\alpha = 0$ in both planes and utilizing

$$\beta_i \geq \left(\frac{\epsilon_i}{\epsilon_r} \right)^{1/2} \beta_r \quad (1)$$

where β and ϵ are the beta function and emittance for the injected beam (i) and ring, respectively. The 95% normalized emittance for the injected beam and final painted emittance are $2.5 \pi\text{-mm-mr}$ and $25 \pi\text{-mm-mr}$, respectively which gives $\beta_i \geq 0.464\beta_r$. For the horizontal, one selects β_i to be equal to $0.464\beta_r$ but in the vertical plane this produces an injected beam with Θ_{\max} too large and the reduced mismatch angle yields to larger number of foil hits. In the vertical, we use a nominal β_r of 27m and β_i of 40m to get the vertical phase space size and orientation properly aligned.

An analytical expression has been developed [10] for the minimum number of foil traversals, h_{\min} , by a circulating beam as

$$h_{\min} = \frac{1}{A} N_i \left(\frac{\epsilon_i}{\epsilon_r} \right)^{1/2} \quad (2)$$

where N_i is the number of injected turns, ϵ is the injected beam emittance, and A in the painted ring emittance.

Simulations

The program STRUCT [11] was utilized to explore the impact of linac current and injection time on the foil hit rate, hit density and peak foil temperature. Table 1 lists the calculated analytical minimum number of hits, h_{\min} , the average hit rate $\langle \# \text{hits} \rangle_{\text{sim}}$ over all six injections, the maximum hit density after the sixth injection, the calculated peak temperature and the nuclear inelastic and nuclear collision loss for the circulating protons. The first three cases show the impact of lengthening injection time on the number of hits, temperature, and losses. The next three investigate reduced vertical injection beta (superscript “R”) and a reduced foil vertical dimension (subscript “s”). The last case looks at CW injection with linac current of 1 mA.

Table 1: Summary of Cases Investigated

case	I	II	III	IV _s	V ^R	VI _s ^R	VII
linac current[mA]	4	2	1	2	2	2	1
pulse length[ms]	1.08	2.16	4.28	2	2	2	25.72
#turns/inj	97	194	385	194	194	385	2310
#turns total	582	1164	2310	1164	1164	1164	2310
h_{\min}	13.5	27.0	53.7	27.0	27.0	27.0	53.7
$\langle \# \text{hits} \rangle_{\text{sim}}$	32.6	60	118	38.7	52.6	45.4	118
hit density _{max} [E12]	34	68	134	64	72	72	515
Peak temp	1090	1480	2050	1420	1520	1520	2320
loss (inelastic) W	93	171	336	110	150	129	336
loss (nuclear coll.) W	65	119	234	77	104	90	234

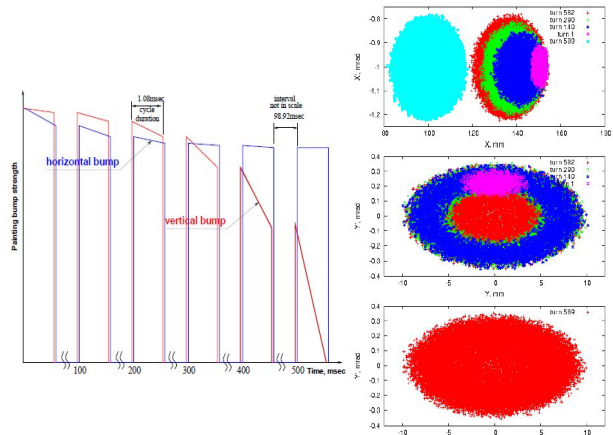


Figure 1: Painting waveform (left) for six injections. Horizontal and vertical phase space distributions (right) during painting process for nominal betas during case I.

The current simulations utilize horizontal painting and vertical angle mismatch at the injection foil (scheme currently used by JPARC) which keeps the foil on the accelerator mid-plane. Note: The painting scheme is not considered optimized and other painting schemes are to be investigated. Figure 1 shows the transverse painting waveform and the evolution of the horizontal and vertical phase space painting through the process. With $\alpha=0$ for both injected and circulation beam assures an upright ellipse and the condition in equation 1 assures a minimum foil size. Figure 2 shows the number of foil hits during each injection. Here case I shows the minimum hits due to shortest injection length where case three (top curve) shows about X4 increase. Comparing case II and IV we see that cutting the foil at $\pm 4\text{mm}$ shows a reduced number of hits, but only a small decrease in peak temperature.

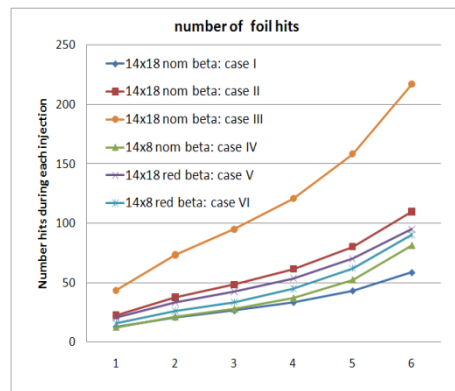


Figure 2: The number of foil hits by the circulating beam during each injection for all cases except the CW case VII.

Figure 3 shows the 2D hit density on the corner foil after the first (left) and last (right) injection. The impact of the injected beam is minimal. Reducing the foil size will reduce foil hits early in the cycle by $\sim 1/2$ but only 5% in the last two injections.

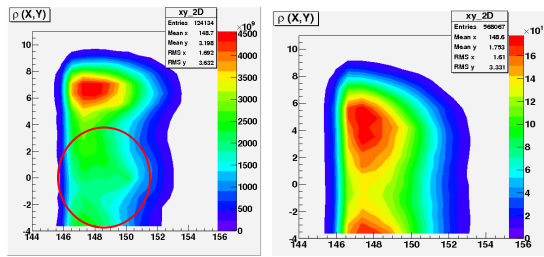


Figure 3: Hit densities on corner foil after the 1st and last injection. The red circle defines the injected beam 6σ size.

Foil Temperature

The hit densities, N , from the STRUCT simulation for each injection are used to calculate the peak temperature as a function of time with

$$\frac{\partial T}{\partial t} = \frac{N}{\rho c(T)} \left| \frac{dE}{dz} \right| - \frac{\epsilon \sigma T^4}{\Delta z} (T^4 - T_0^4) \quad (3)$$

where ρ the density of carbon, $c(T)$ is the specific heat of carbon as a function of temperature, ϵ is the emissivity, σ is the Stephan-Boltzmann constant, and Δz is the foil thickness. The energy deposition term, dE/dz , is modified to reflect the reduction in energy deposition in thin targets due to delta electrons escaping the foil. For 8 GeV protons on a $600 \mu\text{g}/\text{cm}^2$ foil, a simulation with MCNPX shows that approximately 28% of energy is taken away by the delta electrons that escape the foil, thus reducing the energy deposition.

Figure 4 shows the results of the temperature calculation. Note that for the CW case the cooling terms begins to dominate above $\sim 2300^\circ\text{K}$.

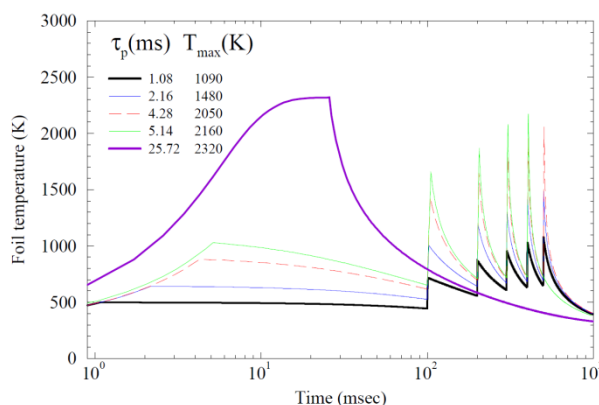


Figure 4: Peak foil temperature for five injection periods. The final accumulated charge is 26 mA-ms for all scenarios.

LASER STRIPPING

The technique of H^+ stripping which avoids the use of a physical foil and its associated issues involves electron photo detachment through a three step process as shown in Figure 5 [12, 13].

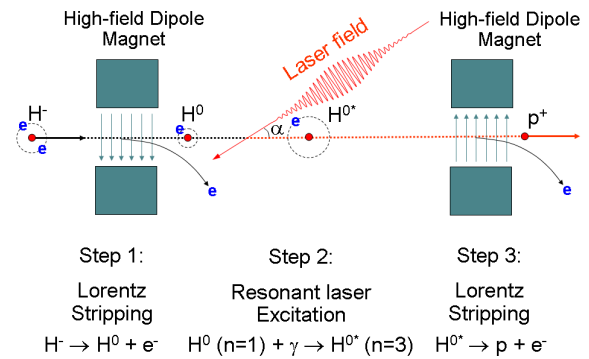


Figure 5: Diagram and explanation of three step stripping scheme [12].

A proof of principal demonstration has been performed at SNS using the resonant laser process (i.e. the hydrogen atom is placed in a laser beam with frequency equal to the transition frequency between the ground and excited state). [14] The excitation takes place in a region shielded from the up and downstream dipoles where $B=0$. The energy spread of the H^0 beam (inherited from the initial H^+ beam) causes each atom in the beam to have its own rest frame excitation frequency. To efficiently excite nearly 100%, requires either a broad-bandwidth laser [15] or a divergent narrow bandwidth laser, which due to the Doppler shift, will present a broad set of frequencies to the H^0 beam. [14]

Estimates of the required laser parameters for laser stripping of 8 GeV H^- into the Recycler for the scheme demonstrated at SNS were performed [16] based upon H^- injection beam parameters attainable for injection into the Recycler are listed Table 2. It should be noted that the minimum micro-bunch duration of 6 ps (rms) corresponds to tracking results (in the 8 GeV linac) in the absence of any linac errors where as the 26 ps (rms) value is the result of tracking with random 1% gradient and 1° phase errors. Estimates of excitation efficiency as a function of laser peak power were performed using a micro bunch duration of 20 ps, for four laser wavelengths with the results shown in Figure 6.

Table 2: H^- Injection Lattice and Beam Parameters

Parameter	Value
Energy	8 GeV
Energy spread (rms)	2.5×10^{-4}
Micro bunch duration (rms)	6 ps (min)
	26 ps (max)
β_x	40 m
β_y	10 m
D and D' (both x and y)	0
$\epsilon_{x,y}$ norm. rms emittance	$0.5 \pi\text{-mm-mr}$

The 1900 nm laser reduces the required peak power by almost a factor of five compared to the 1064 nm light. Although this higher wavelength laser, predominately used in medical and DoD applications, is beginning to mature in development.

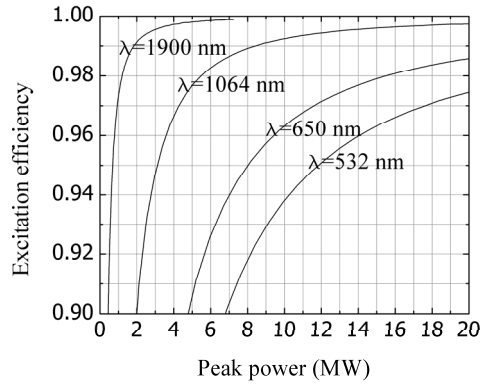


Figure 6: Results of laser power estimation for the case where B field at the interaction point is zero. Curves are for case II below.

Recent advances in the numerical model allow the calculation of the evolution of an H^0 beam taking into account spontaneous emission, field ionization, and external electromagnetic fields have been reported in [17]. This model optimizes the laser parameters as well as the magnetic field strengths and derivatives and magnet geometry with respect to the interaction point. They also consider two different excitation schemes characterized by various magnetic fields and report estimations in a very weak magnetic field and strong magnetic field. For laser stripping in a strong magnetic field, the spectral broadening of the energy levels begins to be comparable with the laser frequency spread in the particle rest frame.

A quantum mechanical model of the hydrogen atom which takes into account the continuum spectrum of the electron and the broadening of its energy levels due to a strong external magnetic field have been reported [18]. A feature of this process is that as the magnetic field (static electric field in the atoms rest frame) increases the Rabi oscillations are attenuated and the population of the ground state decreases as shown in Figure 7. In strong magnetic fields the excitation is followed by immediate ionization.

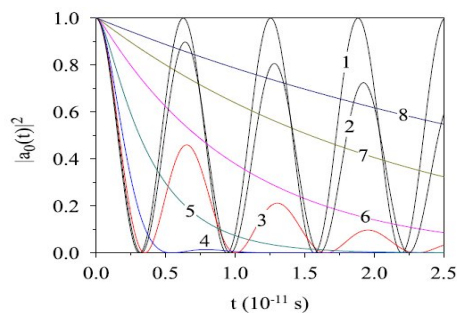


Figure 7: Lifetime of the population of the ground state $|a_0(t)|^2$ for increasing static electric fields [17].

This model was used to estimate required laser parameters for Project X. Table 3 summarizes the laser requirements for 98% stripping for three different

scenarios. The first two scenarios are for a zero magnetic field at the excitation region, with case I being for an elliptical laser beam and case II being for a circular beam. Both cases require a laser divergence to compensate for the spread in resonant frequencies from the finite energy spread in the H- beam. The optimum magnetic field and laser parameters for excitation in a strong magnetic field with a parallel circular laser beam are shown in case III.

Table 3: Required laser parameters for 98% stripping efficiency at 8 GeV. The values in bold are a result of the optimization

Parameter	I	II	III
Incidence angle [deg]		94.6	
Peak power [MW]	5	5.5	10
Micropulse energy [mJ]	0.3	0.4	0.7
Micropulse duration(rms) [ps]		28	
Power at 325 Mhz [kW]	100	130	230
x-rms size [mm]	5.0	2.0	2.0
y-rms size [mm]	1.9	2.0	2.0
X'-divergence [mr]	0.6	0.8	0
Y'-divergence [mr]	0.6	0.8	0
Magnetic field B [T]	0	0	1.1

Implementation Options for Project X

The injection straight section was designed to incorporate both foil stripping and laser stripping techniques. The “stripping foil” could be replaced by the “vertical stripping dipole” and laser interaction region, as shown in Figure 8, with minimal other modifications. The “vertical stripping dipole” is a zero integral dipole which serves to strip the H^- into H^0 with minimal impact on the circulating protons. The position of the laser interaction and the end field requirements is determined by the optimization process.

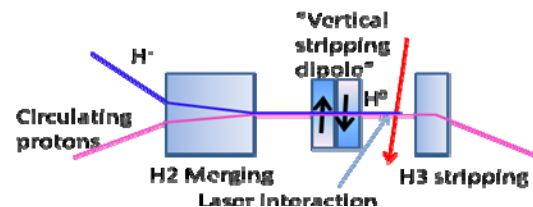


Figure 8: Modification of injection insert to accommodate laser stripping.

The initial investigation of laser techniques will focus on utilizing 1 μ light due to the technological advances in laser sources and optical elements. However, the 1.9 μ light will be investigated as well, although the utilization of YAG dopants such as Ho, Th, and Tm and optical coatings for this wavelength are less well developed.

Basic techniques to supply the required laser power and temporal structure to the interaction are: direct illumination and the use of a build up cavity or recirculation ring. Both techniques will be included in the R&D plan.

Direct Illumination

Direct illumination is an attractive option in that 1) it does not require sensitive optical components to be installed in the accelerator beam pipe and 2) the 325 MHz bunch structure may be encoded at the fiber or semiconductor level using fiber pulse picking technology. In this way laser bursts of MHz micro-pulses with millisecond(s) duration can be created with repetition rates of 10's of hertz. These pulses must be then amplified to the required peak power. Recent advances in cryogenic laser amplifiers [19][20] look promising in creating the desired peak power.

Build-up Cavity

A more conventional method of attaining the required laser power utilizes an optical resonator cavity to build up and store laser power. This cavity must be installed in the accelerator vacuum system such that the H^0 beam crosses the laser path inside the cavity at the appropriate point where the laser beam has the correct geometric (size and divergence) and temporal properties (micro-pulse phase wrt H^0 bunch length). Build up factors of 10's to 100's are possible in laboratory settings, but the required optical coatings must survive in a vacuum and radiation environment. SNS has an active program and are participating with commercial vendors through the SBIR program to develop the required cavity parameters and optics. [21] A hybrid scheme might utilize the amplification of a seed laser to within a factor of 10 of the required laser power and utilize a optical resonant cavity with a modest build up factor of 10.

SUMMARY

One of the central technological issues facing Project X is the H- injection of a low current (i.e. long injection times) H- linac beam into a circular ring using carbon foil stripping technologies is the interaction with circulating beam impacting foil lifetime and losses. The R&D program addresses this issue through investigating potential innovative carbon foil options and the use of laser stripping.

It was shown that a linac with a current of 2 mA and pulse length of 2 ms will satisfy the foil temperature constraint with the assumed painting scheme.

Recent development of cryogenic lasers and laser amplifiers look promising in creating the required laser power.

REFERENCES

- [1] S. Nagaitsev "A Multi-MW proton source at Fermilab", MOPD32, this Workshop (2010).
- [2] Project X ICD -2v2 document, Project X document 648.
- [3] D.E. Johnson "Challenges associated with 8 GeV H- transport and injection for Fermilab Project-X", Proceedings of Hadron Beams 2008, Nashville, Tenn.
- [4] D.E. Johnson, editor, "Conceptual design report of 8 GeV H- transport and injection for the Fermilab Proton Driver", Beams-doc 2597 (March 2008).
- [5] M. Xiao, et. al., "Tune scan with space charge effects for the Recycler ring for Project X", MOPD05
- [6] D. E. Johnson, et. al., "A conceptual design of an internal injection absorber for 8 GeV H- injection into the Fermilab Main Injector", proceedings of Particle Accelerator Conference 2007, Albuquerque, New Mexico, p. 1694.
- [7] D.E. Johnson, "Design of an 8 GeV H- multi-turn injection system for the Fermilab Main Injector", proceedings of Particle Accelerator Conference 2007, Albuquerque, New Mexico, p. 1700.
- [8] S.G. Lebedev, A.S. Lebedev, "Calculation of the lifetimes of thin stripper targets under bombardment of intense pulsed ions", Phys. Rev. ST AB 22, 020401 (2008).
- [9] J. Beebe-Wang, et. al., "Injection mismatch for the SNS accumulator ring", BNL/SNS technical note No. 80 June 1, 2000.
- [10] D. Raparia, "Analytic expression for number of foil traversals", Project X docdb 761 (2009).
- [11] A.I. Drozhdin, et. al., "STRUCT program manual", <http://www-bd.fnal.gov/users/drozhdin/STRUCT>.
- [12] V. Danilov, et. al., "Three-step H- charge exchange injection with a narrow-band laser", Phys. Rev. ST AB 6, 053501 (2003).
- [13] V. Danilov, "Future prospects for laser stripping injection in high intensity machines", Proceedings of Hadron Beams 2008, Nashville, Tenn.
- [14] V. Danilov, et. al., "Proof-of-principle demonstration of high efficiency laser-assisted H- beam conversion to protons", Phys. Rev. ST AB 10, 053501 (2007).
- [15] I. Yamane, "H- charge exchange injection without hazardous stripping foils", Phys. Rev. ST AB 1, 053501 (1998).
- [16] T. Gorlov, "Discussion of the possibility of laser stripping for Project X, Project X docdb 660 (2010).
- [17] T. Gorlov, et. al., "Laser-assisted H- charge exchange injection in magnetic fields", Phys. Rev. St AB 13, 050101 (2010).
- [18] T. Gorlov, et.al., "Effective calculation of laser stripping via a broad shape resonance", Phys. Rev. ST AB (074002 (2010).
- [19] David C. Brown, et. al., "Heat-fraction-limited CW YB:YAG cryogenic solid-state laser with 100% photon-photon efficiency", Optics Express, Vol. 18, Issue 16, pp. 16573-16579 (2010).
- [20] David. C. Brown, et. al., "High sustained average power CW and ultrafast Yb:YAG near-diffraction-limited cryogenic solid-state laser", submitted for publication in Optics Express.
- [21] Phase II SBIR Project, "A laser power build-up system for H atom ionization", Boulder Precision Electro-Optics, Boulder, Co.